

Study of gypsum composite with residue of ornamental rocks: physical, mechanical and thermal analysis

D. C. E. Ferreira^{1*}, J. G. G. de Sousa², N. C. Olivier¹, A. C. S. Dantas¹

¹Universidade Federal do Vale do São Francisco, Programa de Pós-graduação em Ciência dos Materiais, Av. Antônio Carlos Magalhães 510, 48902-300, Juazeiro, BA, Brazil

²Universidade Federal do Vale do São Francisco, Colegiado Engenharia Civil, Juazeiro, BA, Brazil

Abstract

The environmental impacts caused by the disposal of ornamental rock waste require studies for its reuse. Gypsum, a binder widely used in civil construction, can help this recycling process. Thus, some research was carried out in gypsum composites with ornamental rock residue at levels of 0, 5%, 10%, 15%, and 20% and with the water/gypsum (w/g) ratio of 0.6 and 0.8. The properties of setting time, porosity, hardness, compressive strength, thermal conductivity, and tensile bond strength were evaluated. The setting time did not show significant changes for the different contents and w/g ratios. Porosity tended to decrease with the insertion of waste and water decrease. Hardness and compressive strength increased with the inclusion of the residue on the w/g ratio of 0.6. Thermal conductivity and tensile bond strength did not vary greatly.

Keywords: gypsum, waste, ornamental rock, reuse, properties.

INTRODUCTION

Ornamental rocks like granite and marble are commonly used in furniture and building facilities. They are mined as plates, cut, squared, and polished. Common destinations are applications on floors, facades, walls, thresholds, columns, and decorative or functional pieces. Granite and marble are the most common ornamental rocks explored and improved in Brazil. Granites are igneous rocks formed by silicates, basically composed of quartz, feldspar, and mica [1-4]. About 240,000 ton of rock waste is generated per year in Brazil just by cutting and polishing marble and granite [5]. For each cubic meter of sawn rock, a production of 2.2 ton of residue mud is estimated, of which 30% corresponds to rock dust and 67% to water [4]. A large part of this volume of waste is discarded in rivers, ponds, lakes, and streams, causing negative impacts on the environment [2]. Moreover, the excessive extraction of rocks can also accelerate their depletion process, since it is a raw material of natural origin. Civil construction is expected to be an excellent instrument for the recycling process. There are countless fields of application for materials in this sector and studies based on the reuse of waste in binder matrices.

The addition of granite and marble powders in a matrix of high-density polyethylene (HDPE) showed a growth in flexural strength and modulus of elasticity for an addition above 50 wt% [6]. The use of marble and granite mud promoted an increase in consistency in cementitious pastes and an increase in slump, water absorption, and apparent porosity, with a consequent density reduction in concrete samples [7]. The evaluation of self-compacting concrete

produced with marble and granite powders revealed that both residues could be used. For low-strength self-compacting concrete, an addition of up to 360 kg/m³ can be used. High-strength concrete, however, can tolerate an amount of 230 kg/m³. Furthermore, from an adequate moisture correction, the use of marble and granite powders would improve the rheology of the self-compacting concrete without affecting its strength [8]. A study showed that marble and granite waste incorporated into clay used in the production of traditional red ceramics reduced sintering temperature, with less energy consumption and reduced wastage [9]. Coating mortars with granite residue replacing the fine aggregate showed an increase in compressive and bending strength [4].

Gypsum is a mineral composed of calcium sulfate dihydrate that shows great potential as an alternative binder matrix to cement. This material can be used as wall coating in replacement of cementitious mortar, plasterboards, and building blocks. Its great advantages are ease and speed of application, final finishing without the need for layers of another material, lower price compared to cement, and good performance for thermal and acoustic insulation. Considering the available literature, the choice of gypsum and ornamental rock residue for the preparation of a composite was assertive, once the information about the properties of this composite is deficient. Moreover, the easy acquisition, high availability, and low cost of these materials were also incentives for this work. That said, the objective of this research is to produce a composite to reuse the waste ornamental rock through its application as a partial substitute for gypsum in the production of pastes. The work also aims to reduce the environmental impact caused by the disposal of waste and contribute to the study of the physical, mechanical, and thermal properties of gypsum composite with waste ornamental rock. At the same time,

*dceferreira93@outlook.com

 <https://orcid.org/0000-0001-6184-3923>

the results of this research may lead to a greater application of gypsum while maintaining the space already conquered in the market, in addition to opening the way for new research on the subject.

MATERIALS AND METHODS

Obtention of materials: the gypsum used was obtained from the Gypsum Pole of Araripe-PE, Brazil. It is produced by simple calcination of gypsum rocks at approx. 200 °C and available in 40 kg bags. The residue was acquired from a single marble and granite factory located in Juazeiro, Bahia, Brazil. In this factory, the sludge formed during the stone processing was conducted from the cutting table to a pit near the site. When full, this pit was emptied manually by the workers with shovels. At this point, the sludge was collected. In the laboratory, the slurry went directly to an oven, where it remained at 110 °C for 48 h. Finally, the resulting dry material was disintegrated on a 2 mm sieve, without further homogenization.

Characterization of gypsum and ornamental rock waste: the initial characterization of the materials was carried out by X-ray diffraction (XRD), and scanning electron microscopy (SEM) coupled with energy dispersive spectroscopy (EDS). The XRD was performed with a diffractometer (Mini Flex, Rigaku) with a copper radiation source, a voltage of 40 kV, and scan range from 10° to 90° of 2θ angle, angular step of 0.02° and scan speed of 20 °/min. The qualitative analysis of the XRD patterns was performed with the X'Pert HighScore Plus software and the Inorganic Crystal Structure Database (ICSD). For the SEM, a tabletop microscope (TM 1000, Hitachi) was used with coupled EDS (TM 1000X). The samples were analyzed with carbon tape to improve conductivity and metalized with a 120 nm gold layer to improve resolution. An acquisition time of 60 s and acceleration of 15 kV was used. For the SEM and EDS, the TM 1000 and SwiftED-TM software were used, respectively.

Raw material analysis: NBR 13207 standard [10] contains the requirements for characterization, inspection, and acceptance of gypsum to be used in civil construction. Thus, the gypsum acquired for the production of composites was subjected to the characterization of the physical and mechanical requirements according to this standard for the verification of such parameters. The analysis comprised the determination of particle size and unit mass [11], normal consistency and setting time [12], hardness [13], and tensile bond strength [14, 15]. Complementing the information about the gypsum used, the specific mass [16] and the compressive strength [17] were also determined. This stage ended with the analysis of the specific mass and granulometry of the residue using the methodologies already used for gypsum.

Physical and mechanical characterization of composites: at this stage, the study was divided into four steps: fresh state, hardened state, thermal performance, and coating application. The analyzed properties and their methodologies are shown in Table I. Gypsum hardening time varies considerably depending on the proportions of materials used. Therefore,

in the fresh state, testing of this consistency variation of the composites was carried out through the setting time with a Vicat apparatus. Four determinations of each composite were performed to determine the setting time. For the hardened state, the mechanical properties were evaluated by hardness and compressive strength. An analysis of the porosity to better understand the results of the mechanical properties was performed. The porosity (ε) evaluation used the equation:

$$\varepsilon(\%) = \left[1 - \left(\frac{d}{(\%g \cdot d_g) + (\%r \cdot d_r)} \right) \right] \cdot 100 \quad (A)$$

where *d* is the bulk density of the composite, %*g* is the gypsum fraction, *d_g* is the gypsum density, %*r* is the residue fraction, and *d_r* is the residue density; the gypsum and residue densities resulted from the characterization of the materials and the apparent density was calculated considering the mass of the specimen and its geometry. In hardness, three faces of the specimen were subjected to penetration of a sphere of 10.0±0.5 mm in diameter for 15 s with a load of 500±10 N. The penetration depth readings were taken by a caliper to calculate the hardness, *D* (N/mm²), according to:

$$D = \frac{F}{\pi \cdot \phi \cdot t} \quad (B)$$

where *F* is the load (N), *Ø* is the sphere diameter (mm), and *t* is the penetration depth (mm). For compressive strength, the load was applied to one of the side surfaces where the hardness test was not performed, at a constant rate of 2 mm/min, with a load cell capacity of 20 kN, using a testing machine (DL 10000, Emic) and a software (Tesc) in data processing. Three determinations, each with six specimens of 50x50x50 mm, were used for each composite in the determination of porosity, hardness, and compressive strength.

Table I - Assessed properties and testing methodologies.

Property	Methodology
Setting time	NBR 12128 [12]
Hardness	NBR 12129 [13]
Compressive strength	ASTM C472-99 [17]
Thermal conductivity	NBR ISO 8894-1 [18]
Tensile bond strength	NBR 13528-1, 13258-2 [14, 15]

In thermal performance, the thermal conductivity was evaluated by the hot-wire method, which uses the heating of electrical resistance between two specimens in a given time interval. For this, the following were used: a set of blocks with electrical resistance in nickel-chromium wire (Ø 0.50 mm, 5.8 Ω/m, 390 mm length) and type K chromel-alumel thermocouple; an energy source (3003, Instrutherm); a data acquisition board (ADS 2000, Lynx); and a computer equipped with AqDados and AqDados Analysis software. The thermocouple and the datalogger collected and stored

the temperature propagated on the surface of the material and, based on the temperature vs. $\ln(\text{time})$ relation, the thermal conductivity was calculated using Eqs. C and D. Three pairs of blocks, with two readings of 1260 s duration in each pair were tested to determine the thermal conductivity of the composites.

$$\kappa = \frac{q'}{4\pi.t} \quad (\text{C})$$

where κ is the thermal conductivity, q' is the linear power, and τ is the slope of temperature vs. $\ln(\text{time})$;

$$q' = \frac{i^2.R}{l} \quad (\text{D})$$

where i is the electric current (A), R is the electrical resistance (Ω), and l is the wire length (m). Finally, the tensile bond strength between the composite and the wall was evaluated, simulating an application of the gypsum composite paste as an internal coating. In this context, the tensile bond strength of composites was analyzed with the application of coatings on ceramic blocks without roughcast. The ceramic base was prepared individually for each composite and the coating was applied in a single layer using a thickness delimiter, batten, and trowel. After 28 days, cuts were made with a cup saw, 12 per coating, and circular metallic inserts using plastic putty were applied. With the traction equipment connected to the inserts and a dynamometer (Dinateste), the pullout was performed and the tensile bond strength was calculated as the ratio between the pulling force and the area of cut considering the diameter of the specimen. The average of the 12 specimens represented the tensile bond strength of the coating.

The contents of 5%, 10%, 15%, and 20% of mass replacement of gypsum by residue and the water/gypsum (w/g) ratios of 0.6 and 0.8 were selected for the study of the properties described above. For comparative purposes, the pastes without residue were also evaluated using the aforementioned w/g ratios. In Table II, it is possible to visualize the experimental program of the mixtures evaluated according to the variables. The production of pastes and composites shown in Table II began with the weighing of gypsum, waste, and water. Then, the gypsum and the residue were homogenized and sprinkled in water. After this dusting process carried out within a 1 min interval, the mixture was left to rest for 2 min to absorb the water. At the end of this time, the material was mixed for 1 min with the aid of a spatula. Finally, the mixture was sent for evaluation or inserted into the molds for the production of test specimens. This procedure followed ASTM C472-99 [17] and NBR 12128 [12] standards and was adopted for the preparation of pastes and composites for the analysis of all properties. For the production of the thermal test specimens, the dusting time was modified to 3 min, and for the thermal and tensile bond strength analyses, the mixing time used was 2 min. The molded specimens for porosity, hardness, and compressive strength evaluation were placed in an oven at 40 ± 4 °C until reaching constant mass. They were

then placed in a desiccator until the tests were carried out. For the thermal evaluation, the specimens were exposed to room temperature and natural ventilation of the laboratory until constant mass. In the case of coatings, after mixing and applying the pastes/composites, it took 28 days to dry in a laboratory environment. At that moment, the cuts and pasting of the tablets with plastic mass were performed.

RESULTS AND DISCUSSION

Characterization of gypsum and ornamental rock waste

Gypsum powder and dense bodies: the X-ray diffraction pattern of the gypsum powder can be seen in Fig. 1 in comparison to hemihydrate calcium sulfate ($\text{CaSO}_4 \cdot \text{H}_2\text{O}_{0.583}$ - ICSD 79530) and anhydrite (CaSO_4 - ICSD 16382) patterns. So it was possible to confirm the presence of calcium hemihydrate as the main constituent with a small amount of anhydrite. The presence of anhydrite can occur if

Table II - Nomenclature and composition of the samples used in this work.

Sample	w/g ratio	Gypsum (%)	Residue (%)
GR6-0	0.6	100	0
GR6-5	0.6	95	5
GR6-10	0.6	90	10
GR6-15	0.6	85	15
GR6-20	0.6	80	20
GR8-0	0.8	100	0
GR8-5	0.8	95	5
GR8-10	0.8	90	10
GR8-15	0.8	85	15
GR8-20	0.8	80	20

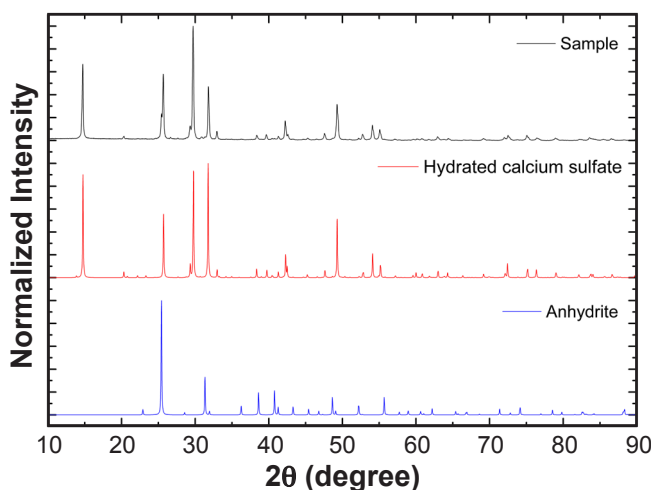


Figure 1: XRD pattern of gypsum powder in comparison to hemihydrate calcium sulfate (ICSD 79530) and anhydrite (ICSD 16382) patterns.

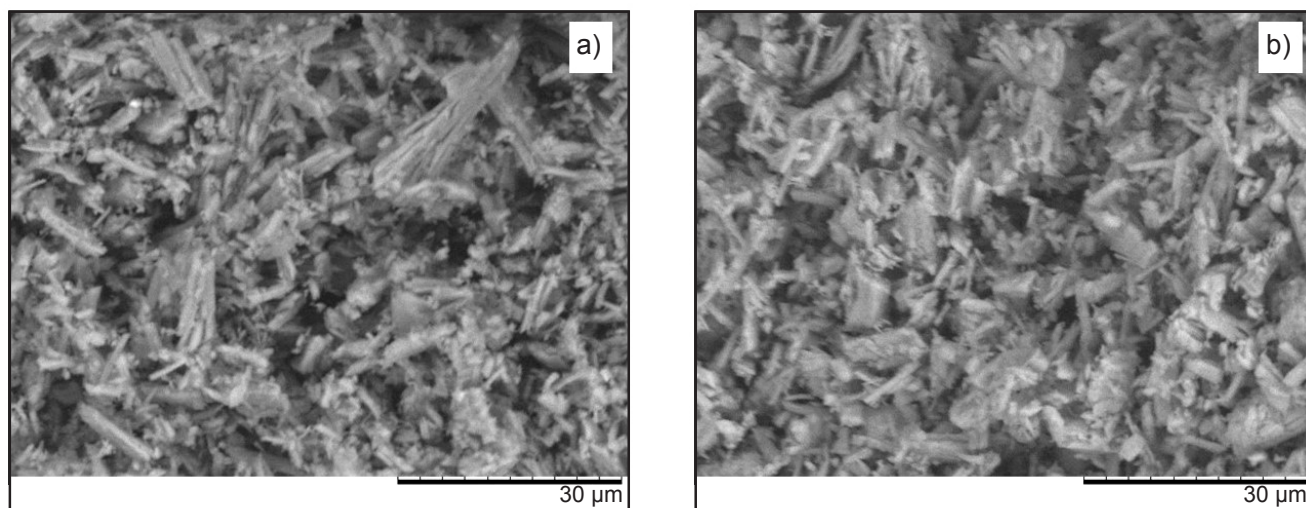


Figure 2: SEM micrographs of the fracture surface of gypsum samples produced with different w/g ratios: a) GR6-0; and b) GR8-0.

Table III - Physical and mechanical requirements of the gypsum used and reference values according to NBR 13207 standard [10].

Property	Result	NBR 13207
Unit mass (kg/m ³)	668±8	≥600.00
Particle size <#0.21 mm (%)	95.5±0.4	≥90.00
Normal consistency (w/g ratio)	0.58	-
Start of setting time (min)	27.4±1.8	≥10.00
End of setting time (min)	35.2±1.0	≥35.00
Hardness (N/mm ²)	37.0±2.3	≥20.00
Tensile bond strength (MPa)	0.57±0.14	≥0.20

w/g: water/gypsum.

during calcination some part of the powder reaches temperatures above 250 °C. The EDS spectrum of gypsum (GR6-0) presented amounts of 62.0 wt% calcium, 37.5 wt% sulfur, 0.3 wt% magnesium and 0.2 wt% silicon. These results are in accordance with the characteristic composition of gypsum. Fig. 2 shows the SEM micrographs of the fracture surface of dense bodies produced with gypsum with different w/g ratios of 0.6 (GR6-0) and 0.8 (GR8-0). In both images, it is possible to see the structure of dehydrated calcium sulfate crystals in the form of intertwined needles, typical of the material [19]. Additionally, it was not observed any difference in crystal sizes and porosity by different w/g ratios. Table III summarizes the physical and mechanical properties of gypsum in comparison with the NBR 13207 standard [10]. The specific mass of the gypsum reached a value of 2.67±0.01 g/cm³ and the compressive strength value of 12.4±0.5 MPa. NBR 13207 standard [10] included this last property as a requirement, in which the samples under characterization should not present values lower than 8.40 MPa as compressive strength, which would put the present gypsum in compliance with the requirement.

Ornamental rock waste: the XRD pattern of the residue is shown in Fig. 3. The XRD peaks of the sample corresponded to silicon oxide (SiO₂ - ICSD 27826), sodium aluminum

silicate (albite, NaAlSi₃O₈ - ICSD 201649), and potassium feldspar (K_{0.5}Na_{0.5}AlSi₃O₈ - ICSD 201602). Silicon oxide and sodium aluminum silicate are the main components of quartz and feldspar, respectively. Therefore, together with the potassic feldspar, they indicate the presence of granite. This result corroborated the compositional variation of the residue already reported in other works: quartz, biotite, albite, anorthite, orthoclase, calcite, dolomite, feldspar, kaolinite, muscovite, and actinolite [4, 7, 9]. The composition of the residue obtained by EDS can be seen in Table IV, reinforcing the compositional variety found in this work and in the literature [4, 6, 7, 9, 20]. The SEM image of the residue can be observed in Fig. 4. It is possible

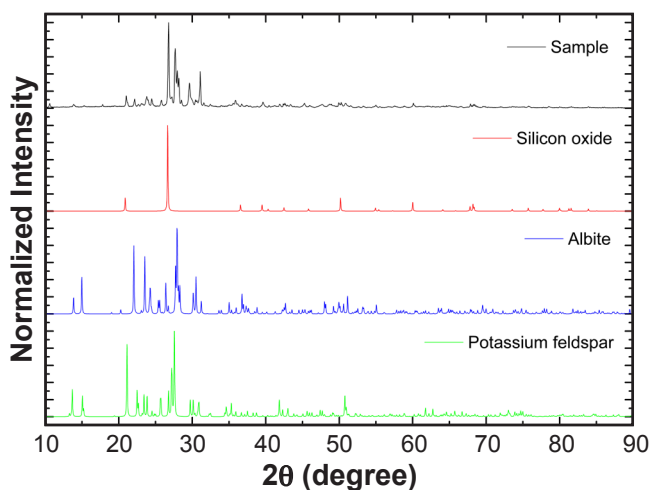


Figure 3: XRD pattern of the residue in comparison to silicon oxide (ICSD 027826), albite (ICSD 201649), and potassium feldspar (ICSD 201602) patterns.

Table IV - Chemical composition (wt%) of pure rock waste obtained by EDS.

Mg	Al	Si	S	K	Ca	Fe
0.4	6.5	27.5	0.1	6.8	24.4	34.4

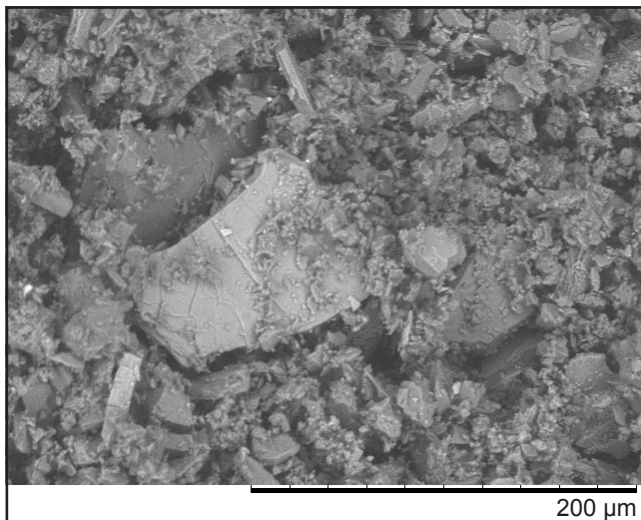


Figure 4: Scanning electron micrograph of pure rock residue.

to visualize the compositional diversity from the different shades of gray obtained by the use of backscattered electrons, and the great variety of shapes and sizes of the particulate. The residue was sieved using a 200 μm sieve, with 94.4%±1.1% of the material passing through it. Subsequently, the specific mass was measured and reached a value of 2.73±0.01 g/cm³.

Physical and mechanical characterization of composites

Setting time: it was not affected by the w/g ratio or residue content (Table V). The start of the setting occurred between 24 and 34 min for the different residue amounts, and the end of the setting time occurred between 30 and 43 min. It was not observed any tendency for the different amounts of residue.

Dense bodies: Fig. 5 shows the measured porosity. The GR8 series presented mean porosity varying between 62.58% and 58.33% while the GR6 series varied between 54.57% and 51.52%. Literature data show apparent porosity indices between 43.5% and 49.5% [21] and between 37% and

Table V - Results of the analysis of the setting time.

Sample	Start setting time (min)	End setting time (min)
GR6-0	28.0±2.3	35.9±3.3
GR6-5	26.7±2.3	36.2±2.3
GR6-10	31.8±2.6	39.4±2.0
GR6-15	24.0±2.1	30.5±1.7
GR6-20	27.9±2.0	33.9±0.8
GR8-0	30.5±0.4	40.2±0.4
GR8-5	34.1±3.9	43.0±3.8
GR8-10	29.9±3.2	37.6±3.7
GR8-15	28.3±2.1	36.6±1.5
GR8-20	28.0±2.7	37.5±3.6

45% after 7 days and between 33% and 39% after 28 days [22]. Fig. 6a shows the results of the hardness analysis.

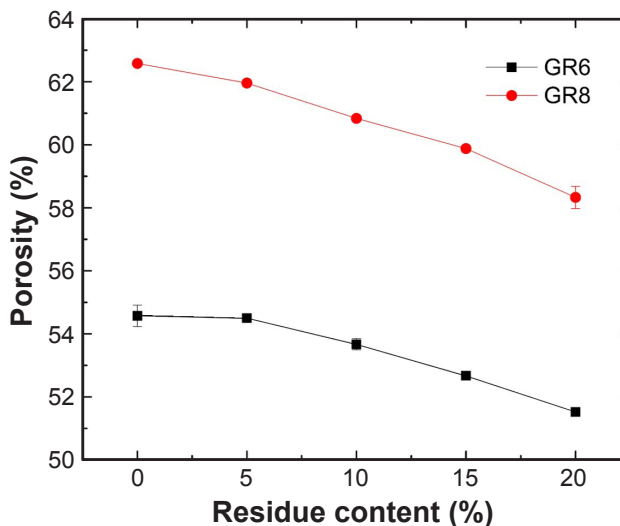


Figure 5: Porosity found in the evaluation of composites with gypsum and ornamental rock residue.

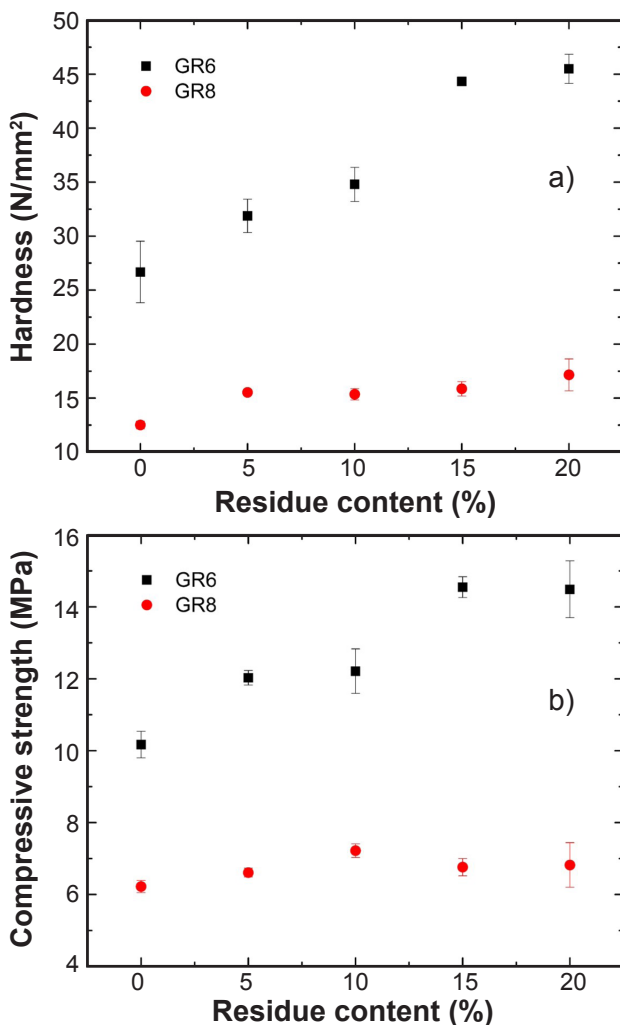


Figure 6: Hardness (a) and compressive strength (b) of composites with gypsum and ornamental rock residue.

The samples presented higher hardness values for the GR6 series. The samples showed also higher values of hardness by higher amounts of residue, independently of the water/gypsum ratio. The GR8 composite with 20 wt% addition showed an increase of 37.09% compared to the samples without residue. For a water/gypsum ratio of 0.6, the variation was more expressive with an increase of 70.50% between the samples without residue and with 20 wt% content of residue. In comparison, the hardness of commercial gypsum samples revealed a value close to 15 MPa [23]. The compressive strength (Fig. 6b) presented a similar behavior, where higher amounts of residue promoted higher values of strength. In samples produced with a w/g ratio of 0.6 (GR6 group), an increase of 43.1% in the compressive strength could be observed by the addition of 15 wt% of residue. Samples of the GR8 group showed the same behavior but with a lower increase in compressive strength. These samples reached an increase of 16.1% with the addition of 10 wt% of residue.

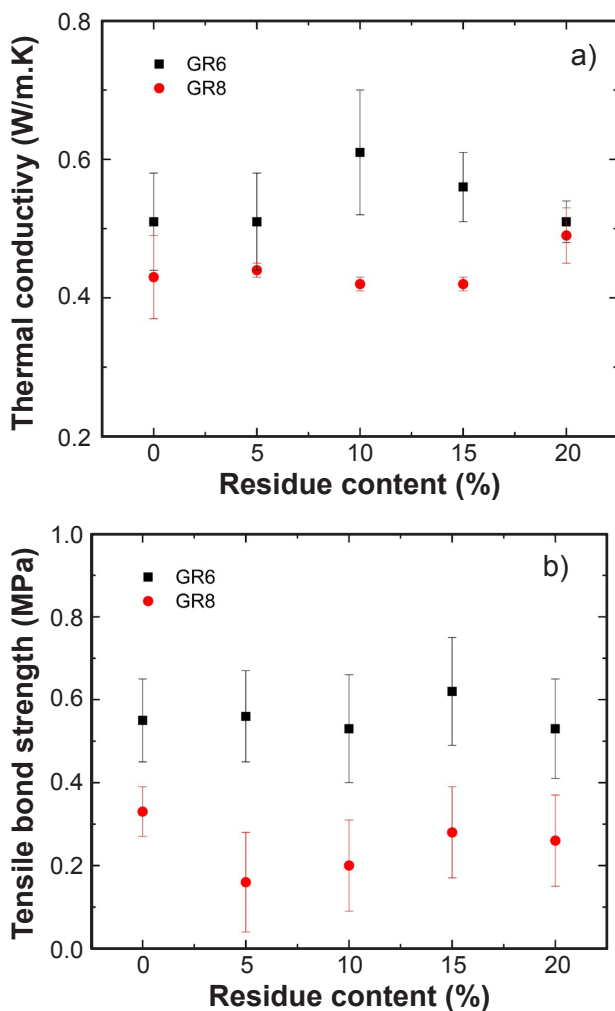


Figure 7: Thermal conductivity (a) and tensile bond strength (b) of the GR6 and GR8 samples as a function of the amount of rock waste introduced.

Thermal performance: the thermal conductivity of the bodies can be seen in Fig. 7a. The thermal conductivity of the samples produced with a w/g ratio of 0.6 reached values between 0.507 ± 0.029 and 0.614 ± 0.060 W/(m.K). The samples produced with a w/g ratio of 0.8 reached thermal conductivities between 0.422 ± 0.012 and 0.493 ± 0.040 W/(m.K) for different amounts of residue. Thermal conductivity values between 0.384 and 0.497 W/(m.K) were found in the literature involving gypsum [24]. Indices of 0.4707, 0.3361, 0.3011, and 0.2537 W/(m.K), the first referring to pure gypsum and the others to the different contents of micro encapsulates were also reported [25].

Coating application: Fig. 7b presents the tensile bond strength for all samples. Samples produced with a w/g ratio of 0.6 presented higher strengths than samples produced with a w/g ratio of 0.8. Samples produced with higher water amounts reached a maximum bond strength of 0.33 ± 0.06 MPa, while samples produced with a w/g ratio of 0.6 reached bond strength values between 0.53 ± 0.12 and 0.62 ± 0.13 MPa. No significant variation of the bond strength was observed for the different amounts of residue, independent of the w/g ratio used. The literature data on tensile bond strength shows values between 0.20 and 0.60 N/mm², also showing great variety [26]. In another work [27], five different types of plaster from the Pole of Araripe-PE, Brazil, were evaluated. These samples reached bond strength between 0.37 ± 0.14 and 0.54 ± 0.17 MPa.

SEM and EDS analyses of composites: Figs. 8a and 8b refer to the composite GR6-20. The highlight in the image represents the waste particles, with a different shape from the needle structure. In Figs. 8c and 8d, the microstructure of composite GR8-20 is represented. The differences in color and shape of the residue in relation to the gypsum matrix are clear, whose structure was maintained occurring only insertion of the particulate in its environment. Table VI shows the EDS results for GR6-20 and GR8-20. As expected, the data demonstrated the predominance of calcium and sulfur, presenting both in the pure residue and in the binder matrix, with a smaller amount of magnesium, aluminum, silicon, potassium, and sodium.

Explanation of the obtained results: the maintenance of the setting time results would be due to an inert behavior of the residue. Its particles would not be interacting with the gypsum during hydration, saturation, precipitation, and crystal formation processes. That is, the residue would not function as a crystallization nucleus, in order to accelerate the reactions, nor as a retarding agent, capable of delaying such processes. Thus, its role would be related to functioning as an inert graft dispersed in the medium in which the entire setting process related to the gypsum takes place. In addition, the water/gypsum ratio was kept fixed throughout the replacement of gypsum by residue and the intervals between the beginning and end of setting were very close to each other, reaching values between 6 and 10 min for all the mixtures analyzed. These two points reinforced the idea of waste as an inert graft. Finally, it was possible to observe in the SEM images that the residue fragments did not present

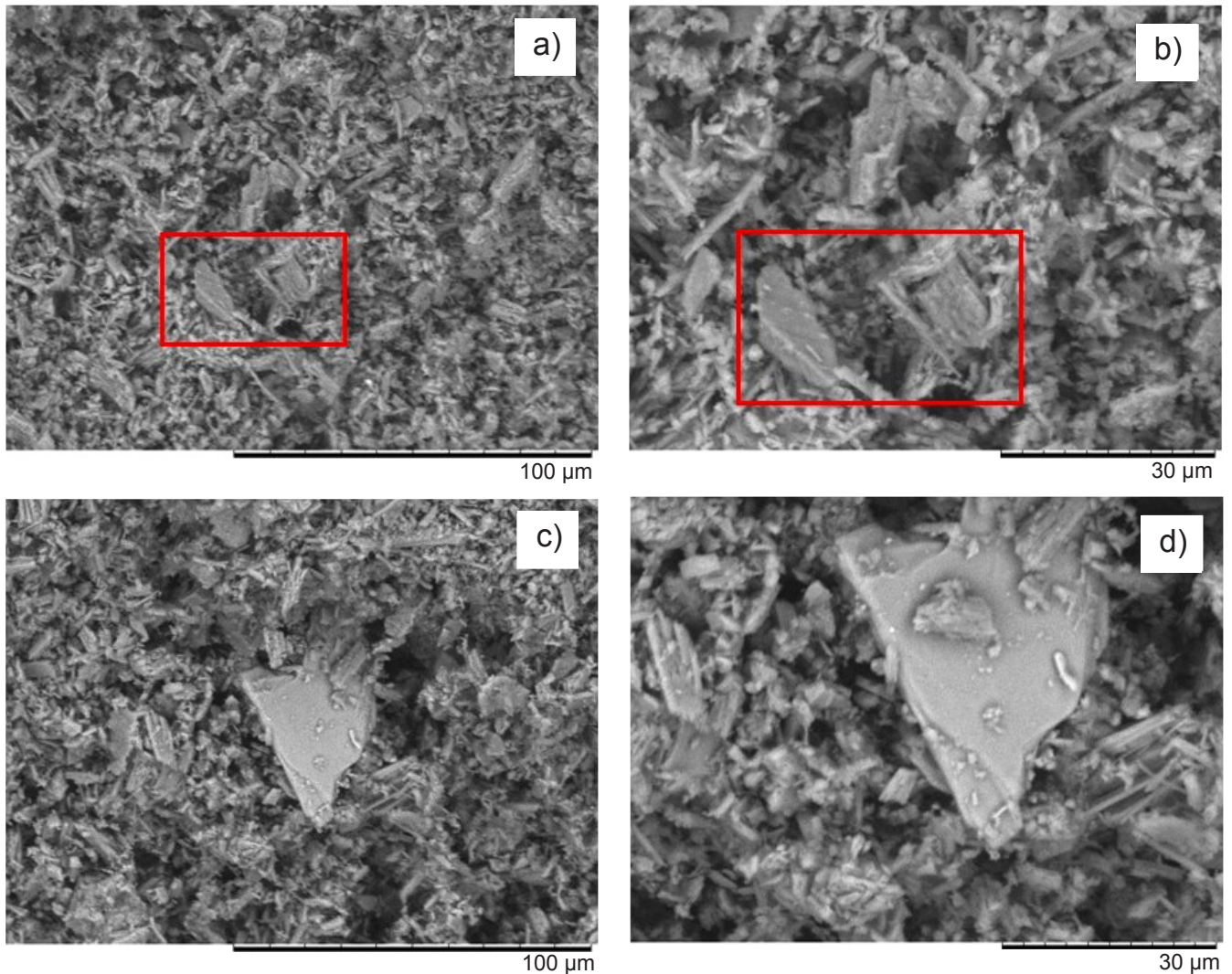


Figure 8: Scanning electron micrographs of composites at different magnifications: a,b) GR6-20; and c,d) GR8-20.

Table VI - Chemical compositions (wt%) of the GR6-20 and GR8-20 composites obtained by EDS.

Composite	Mg	Al	Si	S	K	Ca	Fe
GR6-20	0.1	1.7	1.3	34.7	1.1	61.2	-
GR8-20	0.4	3.2	2.1	33.9	-	59.3	1.0

gypsum crystals on their surface, reinforcing once again the inert graft behavior and justifying the maintenance of the setting results.

As for the analysis of dense bodies, during the drying process of pastes and composites, water not used in the hydration process is eliminated. In their place, voids or pores appear. Thus, the greater the amount of water used, the greater the amount of pores formed. Therefore, higher porosity indices were verified with mixtures produced with a water/gypsum ratio of 0.8. With the increasing replacement of gypsum by the residue, it was noticed that there was also a decrease in porosity. In this case, as the water/gypsum ratio was kept fixed, there was no change in its amount based

on gypsum, even though the proportion of dry materials increased as the residue content increased. But, put in this way, the general amount of water present in the mixture, responsible for promoting the mixing of the gypsum and the residue, decreased during the replacements. This led to an understanding of the porosity reduction observed as waste was added to the mixtures. This decrease in porosity had a direct impact on hardness and compressive strength indices. As expected, the smaller amount of water in GR6 promoted higher hardness and compressive strength values compared to GR8 due to the lower values of porosity. The greater amount of water in the GR8 set promoted the formation of a greater number of pores after drying. These pores acted as stress concentrators in ceramic materials, intensifying the load and providing breakage at lower loads, reducing strength. The shape of the pore, the distance between two or more pores, and between the surface and the pore also directly affect the hardness and strength values. Considering a pore that is close to the surface, the material that separates them can end up breaking first and creating a flaw whose size encompasses the pore itself along with the extension of

the material that separates it from the surface, reducing the mechanical resistance. The same can be thought of several nearby pores, which can unite in a larger failure from the precipitated rupture of the material that separates them, and thus decrease the total strength [28, 29]. Furthermore, when the water/gypsum ratio was reduced in the two series with the replacement by residue, the hardness and compressive strength showed greater changes in the w/g ratio of 0.6 probably because the amount of water still remained high with w/g ratio being 0.8, so that the increase in waste was not significant.

In thermal analysis, once again, the main issue of this behavior seemed to be the amount of water used in the production of the composite. As discussed, there was an increase in porosity in the GR8 series composites, which directly affected, among other factors, the thermal conductivity [30-32]. The space left by these pores was filled with air, which made it difficult to conduct heat internally, reducing the property of the GR8 set as a whole compared to the GR6 series [29]. As for the residue, its insertion in different contents caused a change in the porosity which was not enough to modify the thermal conductivity of the material, maintaining the conductivity range of gypsum materials. And, even the residue coming from the granite, a rock with thermal conductivity of 3.5 W/(m.K), there were not any property changes in the final composite [33]. Finally, the insertion of the residue was not enough to modify the adhesion mechanisms of the coating to the substrate. Again, the small variation in the results was associated with the amount of water used.

CONCLUSIONS

The setting time analysis revealed that the insertion of up to 20% of the residue in gypsum did not cause significant changes. With this, it is believed that the residue did not undergo any reaction during the hydration, saturation, and precipitation processes inherent to gypsum and that it functioned as an inert graft. In addition, the SEM micrographs did not reveal gypsum crystals adhered to the waste particles, reinforcing the non-participation of waste in these processes and in crystal growth. Porosity was higher in mixtures produced with a water/gypsum ratio of 0.8 due to the greater amount of pores formed after drying. There was also a reduction in porosity as the residue content in the mixtures increased. This behavior was related to the decrease in the amount of water used during the insertion of the residue since the water/gypsum (w/g) ratio was kept fixed. The smaller amount of pores formed with the insertion of the residue and with the use of smaller amounts of water provided a significant increase in hardness and compressive strength for mixtures with a w/g ratio of 0.6. As the pores function as stress concentrators and strength reducers, the indices for w/g of 0.8 were lower and with inexpressive growth. This reduction in porosity decreases the voids filled with air, which characterizes a medium of low thermal conductivity. However, it did not reach sufficient levels to

affect the thermal conductivity when it came to the variation of the residue content. The main change in this property was due to the amount of water used when changing the w/g ratio from 0.6 to 0.8 so that the latter had more pores and slightly lower conductivity indices. As for the tensile bond strength, the results demonstrated that there was no change in the adhesion of the coating to the substrate when it came to changing the residue content. And, even with the modification of the w/g ratio, considerable variations in the tensile adhesion strength indexes were not noticed.

REFERENCES

- [1] A.M.A. Santos, R.Z.L. Cançado, R.M. Anjos, N.C. Amaral, L.C.A. Lima, *Rev. Bras. Saúde Ocup.* **32**, 116 (2007) 11.
- [2] T.F. Almeida, F.H.G. Leite, J.N.F. Holanda, in *I Enc. Eng. Ciên. Mater. Inov. Est. Rio Janeiro*, Rio Janeiro (2015).
- [3] A.B. Luz, F.A.F. Lins, *Rochas & minerais industriais: usos e especificações*, CETEM/MCT (2008).
- [4] A.S. Nascimento, C.P. Santos, F.M.C. Melo, V.G.A. Oliveira, R.M.P.B. Oliveira, Z.S. Macedo, H.A. Oliveira, *J. Clean. Prod.* **265** (2020) 121808.
- [5] R. Kumayama, M.A.M. Alcântara, W.S. Cruz, A.A.S. Segantini, *Rev. Eletr. Eng. Civil* **10**, 2 (2015) 56.
- [6] A.H. Awad, R. El-Gamasy, A.A.A. El-Wahab, M.H. Abdellatif, *Ain Shams Eng. J.* **11** (2020) 1211.
- [7] M.A. Rashwan, T.M. Al-Basiony, A.O. Mashaly, M.M. Khalil, *J. Build. Eng.* **32** (2020) 101697.
- [8] M. Meera, Anuj, A.K. Dash, S. Gupta, *Mater. Today Proc.* **32** (2020) 1005.
- [9] W. Acchar, F.A. Vieira, D. Hotza, *Mater. Sci. Eng. A* **419** (2006) 306.
- [10] ABNT, NBR 13207, “Gesso para construção civil: requisitos”, Ass. Bras. Normas Técn., Rio Janeiro (2017).
- [11] ABNT, NBR 12127, “Gesso para construção: determinação das propriedades físicas do pó”, Ass. Bras. Normas Técn., Rio Janeiro (2019).
- [12] ABNT, NBR 12128, “Gesso para construção: determinação das propriedades físicas da pasta”, Ass. Bras. Normas Técn., Rio Janeiro (2019).
- [13] ABNT, NBR 12129, “Gesso para construção civil: determinação das propriedades mecânicas”, Ass. Bras. Normas Técn., Rio Janeiro (2019).
- [14] ABNT, NBR 13528-1, “Revestimento de paredes de argamassas inorgânicas: determinação da resistência de aderência à tração, parte 1: requisitos gerais”, Ass. Bras. Normas Técn., Rio Janeiro (2019).
- [15] ABNT, NBR 13528-2, “Revestimento de paredes de argamassas inorgânicas-determinação da resistência de aderência à tração, parte 1: aderência ao substrato”, Ass. Bras. Normas Técn., Rio Janeiro (2019).
- [16] ABNT, NBR 16605, “Cimento Portland e outros materiais em pó: determinação da massa específica”, Ass. Bras. Normas Técn., Rio Janeiro (2017).
- [17] ASTM, C472-99, “Standard test methods for physical testing of gypsum, gypsum plasters and gypsum concrete”,

Am. Soc. Test. Mater., West Conshohocken (2014).

[18] ABNT, NBR ISO 8894-1, “Materiais refratários: determinação da condutividade térmica, parte 1: métodos do fio-quente (arranjo cruzado e termômetro de resistência)”, Ass. Bras. Normas Técn., Rio Janeiro (2014).

[19] K.S. Babu, C. Ratnam, *Mater. Today Proc.* **44** (2021) 2245.

[20] S. Ghorbani, I. Taji, M. Tavakkolizadeh, A. Davodi, J. Brito, *Constr. Build. Mater.* **185** (2018) 110.

[21] H.A. Moghadam, A. Mirzaei, *J. Build. Eng.* **28** (2020) 101075.

[22] A.A. Khalil, A. Tawfik, A.A. Hegazy, M.F. El-Shahat, *Constr. Build. Mater.* **68** (2014) 580.

[23] G. Camarini, M.C.C. Pinto, A.G. Moura, N.R. Manzo, *Constr. Build. Mater.* **124** (2016) 383.

[24] O. Gencil, J.J.C. Diaz, M. Sutcu, F. Koksall, F.P.A. Rabanal, G. Martínez-Barrera, *Constr. Build. Mater.* **113** (2016) 732.

[25] Y. Zhang, W. Tao, K. Wang, D. Li, *Renew. Energy* **149**

(2020) 400.

[26] M.R. Merino, J.S.C. Astorqui, P.V. Sáez, R.S. Jiménez, M.G. Cortina, *Constr. Build. Mater.* **158** (2018) 649.

[27] F.C. Ferreira, J.G.G. Sousa, A.M.P. Carneiro, *Amb. Constr.* **19**, 4 (2019) 207.

[28] V.M. John, M.A. Cincotto, *Materiais de construção civil e princípios de ciência e engenharia de materiais*, IBRACON (2010).

[29] D.W. Richerson, *Modern ceramic engineering: properties, processing, and use in design*, Taylor Francis (1992).

[30] J. Sundberg, P. Back, L.O. Ericsson, J. Wrafter, *Int. J. Rock Mech. Min. Sci.* **46**, 6 (2009) 1023.

[31] I. Rahmanian, Y.C. Wang, *Constr. Build. Mater.* **26**, 1 (2012) 707.

[32] E.R.H. Figueiredo, A.C. Galindo, J.A.M. Moreira, F.A.P.L. Lins, *Rev. Bras. Geo.* **26**, 3 (2008) 293.

[33] A.B. Frota, S.C. Schiffer, *Manual de conforto térmico*, Studio Nobel (2001).

(*Rec. 11/10/2022, Rev. 22/04/2023, Ac. 04/06/2023*)

